J|A|C|S
ARTICLES

Published on Web 12/29/2008

Giant Dendritic Molecular Electrochrome Batteries with Ferrocenyl and Pentamethylferrocenyl Termini

Catia Ornelas, Jaime Ruiz, Colette Belin, and Didier Astruc*

Institut des Sciences Moléculaires, UMR CNRS 5255, Université Bordeaux 1, 351 Cours de la Libération, 33405 Talence Cedex, France

Received August 7, 2008; E-mail: d.astruc@ism.u-bordeaux1.fr

Abstract: Giant redox dendrimers were synthesized with ferrocenyl and pentamethylferrocenyl termini up to a theoretical number of 3^9 tethers (seventh generation). Lengthening of the tethers proved to be a reliable strategy to overcome the bulk constraint at the dendrimers periphery. These redox metallodendrimers were characterized by ^{1}H, ^{13}C, and ^{29}Si NMR; MALDI-TOF mass spectrometry (for the low generations); elemental analysis; UV−vis spectroscopy; dynamic light scattering (DLS); atomic force microscopy (AFM); electron-force microscopy (EFM) for half- or fully oxidized dendrimers; cyclic voltammetry; and coulometry. UV−vis spectroscopy, coulometry, and analytical data are consistent with an increasing amount of defects as the generation number increases, with this amount remaining relatively weak up to G_5. AFM shows that the dendrimers form aggregates of discrete size on the mica surface, recalling the agglomeration of metal atoms in monodisperse nanoparticles. Cyclic voltammetry reveals full chemical and electrochemical reversibility up to G_7, showing that electron transfer is fast among the flexible peripheral redox sites. Indeed, the redox stability of these new electrochromic dendrimers, i.e., a battery behavior, was established by complete chemical oxido-reduction cycles, and the blue 17-electron ferrocenium and deep-green mixed-valence Fe(III)/Fe(II) dendritic complexes were isolated and characterized. AFM studies also show the reversible dendrimer size changes from upon redox switching between Fe(II) and Fe(III), suggesting a breathing mechanism controlled by the redox potential. Considerable adsorption of high-generation dendrimers on Pt electrodes such as G_7-Fc allows the easy formation of modified electrodes that sense the ATP anion only involving the electrostatic factor even in the absence of any other type of interaction with the redox tethers.

Introduction

Dendrimers[1] have numerous potential applications in biology,[2] catalysis[3] and materials science.[4] The richness of the physical properties found in organometallic (in particular ferrocenyl) polymers[5] encouraged chemists to introduce organometallic complexes into the dendritic structure in order to obtain well-defined macromolecules with interesting physical properties.[1−4] In particular, metallocenyl dendrimers[6] have already been applied in redox sensing[7a−c] and various types of catalysis.[7d−h]

Although dendrimer science is now well-spread,[1] only a few syntheses and characterizations of large dendrimers have been reported.[8] The seminal synthesis of PAMAM dendrimers by Tomalia[8b−d] and his group in the early 1980s was a remarkable landmark, however, in terms of very large dendrimers.[8a−c] Our

(1) (a) Newkome, G. R.; Moorefield, C. N.; Vögtle, F. *Dendrons and Dendrimers. Concepts, Synthesis and Applications*; Wiley-VCH, Weinheim, Germany, 2001. (b) *Dendrimers and Other Dendritic Polymers*; Tomalia, D., Fréchet, J. M. J., Eds.; Wiley-VCH: New York, 2002. (c) *Dendrimers and Nanosciences*; Astruc, D., Ed.; Elsevier: New York, 2003; Vol. 6, pp 709−1208; (d) Reviews on metallodendrimers: Newkome, G. R.; He, E.; Moorefield, C. N. *Chem. Rev.* **1999**, *99*, 1689–1746. (e) Hwang, S. H.; Shreiner, C. D.; Moorefield, C. N.; Newkome, G. R. *New J. Chem.* **2007**, *31*, 1192–1217.

(2) (a) Astruc, D. *C. R. Acad. Sci.* **1996**, *322*, 757–766, Sér. II *b.* (b) Kojima, C.; Kono, K.; Maruyama, K.; Takagishi, T. *Bioconjugate Chem.* **2000**, *11*, 910–917. (c) Hecht, S.; Fréchet, J. M. J. *Angew.Chem., Int. Ed.* **2001**, *40*, 74–91. (d) Sadler, K.; Tam, J. P. *J. Biotechnol.* **2002**, *90*, 195–205. (e) Cloninger, M. J. *Curr. Opin. Chem. Biol.* **2002**, *6*, 742–748. (f) Stiriba, S. E.; Frey, H.; Haag, R. *Angew. Chem., Int. Ed.* **2002**, *41*, 1329–1334. (g) Grinstaff, M. W. *Chem.—Eur. J.* **2002**, *8*, 2838–2846. (h) Boas, U.; Heegarard, P. M. H. *Chem. Soc. Rev.* **2004**, *33*, 43–63. (i) Lee, C.; Mac Kay, J. A.; Fréchet, J. M. J.; Szoka, F. *Nat. Biotechnol.* **2005**, *23*, 1517–1526.

(3) (a) Oosterom, G. E.; Reek, J. N. H.; Kamer, P. C. J.; van Leeuwen, P. W. N. M. *Angew. Chem., Int. Ed.* **2001**, *40*, 1828–1849. (b) Astruc, D.; Chardac, F. *Chem. Rev.* **2001**, *101*, 2991–3024. (c) Kreiter, R.; Kleij, A. W.; Klein Gebbink, R. J. M.; van Koten, G. In *Dendrimers IV: Metal Coordination, Self Assembly, Catalysis*; Vögtle, F., Schalley, C. A., Ed.; Topics in Current Chemistry; Springer-Verlag: Berlin, 2001' Vol. 217, p 163. (d) van Heerbeeck, R.; Kamer, P. C. J.; van Leeuwen, P. W. N. M.; Reek, J. N. H. *Chem. Rev.* **2002**, *102*, 3717–3756. (e) Liang, C.; Fréchet, J. M. J. *Prog. Polym. Sci.* **2005**, *30*, 385. (f) Méry, D.; Astruc, D. *Coord. Chem. Rev.* **2006**, *250*, 1965–1979.

(4) (a) Zeng, F.; Zimmerman, S. C. *Chem. Rev.* **1997**, *97*, 1681–1712. (b) Matthews, O. A.; Shipway, A. N.; Stoddart, J. F. *Prog. Polym. Sci.* **1998**, *23*, 1–56. (c) Venturi, M.; Serroni, S.; Juris, A.; Campagna, S.; Balzani, V. In *Dendrimers*; Vögtle, F., Ed.; Topics in Current Chemistry; Springer-Verlag: Berlin, 1998; Vol. 197, pp 193−228; (d) Bosman, A. W.; Bruining, M. J.; Kooijman; Spek, A. L.; Janssen, R. A. J.; Meijer, E. W. *J. Am. Chem. Soc.* **1998**, *120*, 5547–8548. (e) Bosman, A. W.; Janssen, H. M.; Meijer, E. W. *Chem. Rev.* **1999**, *99*, 1665–1688. (f) Grayson, S. M.; Fréchet, J. M. J. *Chem. Rev.* **2001**, *101*, 3819–3867. (g) Crooks, R. M.; Zhao, M.; Sun, L.; Chechik, V.; Yeung, L. K. *Acc. Chem. Res.* **2001**, *34*, 181–190.

(5) (a) Foucher, D. A.; Tang, B. Z.; Manners, I. *J. Am. Chem. Soc.* **1992**, *114*, 6246–6248. (b) Manners, I. *Advan. Organomet. Chem.* **1995**, *37*, 131–168. (c) Nguyen, P.; Gomez-Elipe, P.; Manners, I. *Chem. Rev.* **1999**, *99*, 1515–1548. (d) Whittell, G. R.; Manners, I. *Adv. Mater.* **2007**, *19*, 3439–3468. (e) Eloi, J. C.; Chabanne, L; Whittell, G. R.; Manners, I. *Mater. Today* **2008**, *11*, 28–36.

10.1021/ja8062343 CCC: $40.75

Scheme 1. Schematic Representation of the Tether-Lengthening Strategy for the Introduction of Bulky Functional Groups at the Periphery of Large Dendrimers

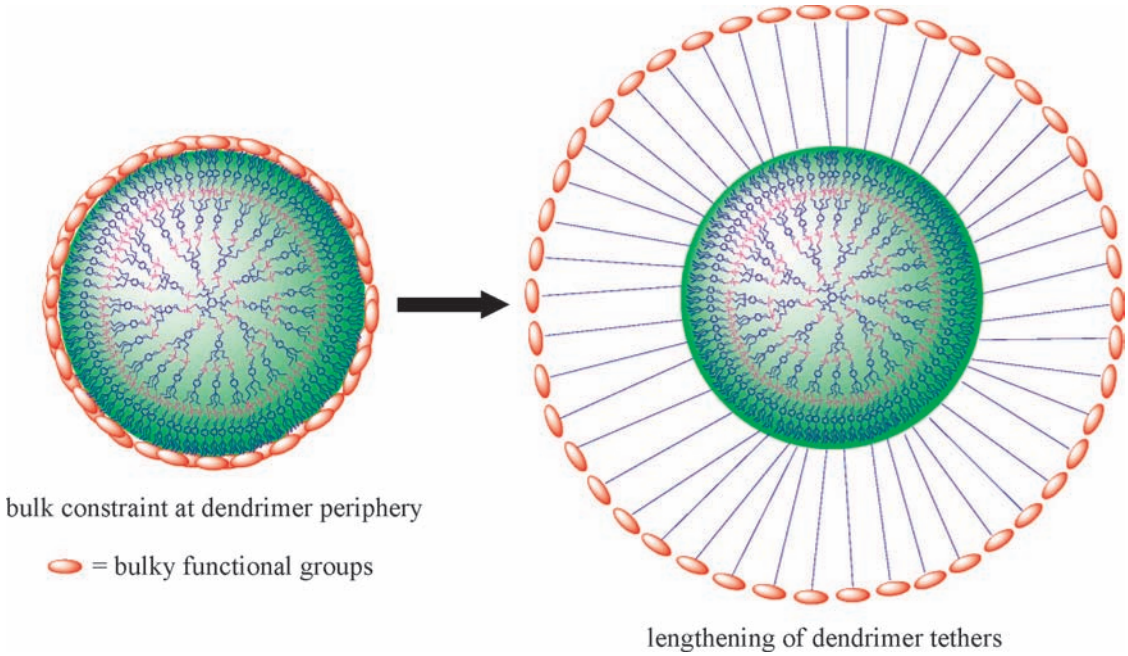

group has recently described the synthesis and characterizations of giant organic dendrimers utilizing an organo-iron synthetic route.[9] Our efforts are now focusing on the functionalization of such dendrimers with robust redox groups, in order to investigate whether a limit to redox reversibility is attained for large dendrimers and to forecast applications in the nanoelectronics field.

The functionalization of dendrimers requires clean and quantitative reactions to avoid the formation of mixtures among the branch termini. Low-generation dendrimers can be functionalized by classic reactions, but giant dendrimers require special attention due to the bulk constraint at the periphery. Indeed, it has been proposed that backfolding of dendritic termini is all the less pronounced as these terminal groups are bulkier.[10c,d] Although the synthesis of ferrocenyl dendrimers has been reported by various research groups,[11] the introduction of bulky organometallic complexes at the termini of the branches of giant dendrimers remains a challenge. We now show that lengthening of the dendrimers tethers is a reliable strategy to overcome these steric problems (Scheme 1).

The strategy of lengthening the dendrimer tethers was applied by attaching a long alkyl chain to the metallocene followed by its reaction with the dendrimers. The syntheses, characterizations, and remarkable physical properties of the resulting ferrocenyl and pentamethylferrocenyl dendrimers are detailed in this article.

Results and Discussion

1. Synthesis of the Organic Dendrimers. The dendritic construction of the dendritic cores follows the known procedure shown in Scheme 2 illustrating the multiplication by three of the number of terminal allyl groups, generations being built up by sequences involving Williamson reaction followed by hydrosilylation.[9]

2. Functionalization of the Dendrimers with Redox-Active Termini. In order to search applications in the nanoelectronics field, such as molecular batteries[12a−d] or capacitors,[12e−g] robust

(6) (a) For a review on ferrocenyl dendrimers and their electrochemical properties, see: Casado, C. M.; Cuadrado, I.; Moran, M.; Alonso, B.; Garcia, B.; Gonzales, B.; Losada, J. *Coord. Chem. Rev.* **1999**, *185*−*186*, 53–79. (b) For electrochemical studies of ferrocenes, see: Holloday, J. D. L.; Bowden, W. L.; Geiger, W. E. *J. Am. Chem. Soc.* **1977**, *99*, 7089–7090. (c) Holloday, J. D. L.; Geiger, W. E. *J. Am. Chem. Soc.* **1979**, *101*, 2038–2044. (d) For electrochemical studies of multi-ferrocenyl oligomers and polymers, see Rulkens, R.; Lough, A.-J.; Manners, I.; Lovelace, S. R.; Grant, C.; Geiger, W. E. *J. Am. Chem. Soc.* **1996**, *118*, 12683–12695. (e) Camine, N.; Mueller-Westerhoff, U. T.; Geiger, W. E. *J. Organomet. Chem.* **2001**, *637*, 823–826.

(7) (a) Valério, C.; Fillaut, J.-L.; Ruiz, J; Guittard, J.; Blais, J.-C.; Astruc, D. *J. Am. Chem. Soc.* **1997**, *119*, 2588–2589. (b) Casado, C. M.; Cuadrado, I.; Alonso, B.; Morán, M.; Losada, J. *J. Electroanal. Chem.* **1999**, *463*, 87–92. (c) Astruc, D.; Daniel, M.-C.; Ruiz, J. *Chem. Commun.* **2004**, 2637–2649. (d) Rigaut, S.; Delville, M.-H.; Astruc, D. *J. Am. Chem. Soc.* **1997**, *119*, 11132–11133. (e) Albrecht, M.; Hovestad, N. J.; Boersma, J.; van Koten, G. *Chem.—Eur. J.* **2001**, *7*, 1289–1294. (f) Daniel, M.-C.; Astruc, D. *Chem. Rev.* **2004**, *104*, 293–346. (g) Ornelas, C.; Ruiz, J.; Cloutet, E.; Alves, S.; Astruc, D. *Angew. Chem., Int. Ed.* **2007**, *46*, 872–877. (h) Astruc, D.; Ornelas, C.; Ruiz, J. *Acc. Chem. Res.* **2008**, *41*, 841–856.

(8) (a) de Gennes, P.-G.; Hervet, H. *J. Phys., Lett.* **1983**, *44*, L351–360. (b) Denkewalker, R. G.; Kolc, J. F.; Lukasavage, W. J. U.S. Patent 1983 4410688; *Chem. Abstr.* **1984**, *100*, 103907. (c) Tomalia, D. A.; Baker, H.; Dewald, J. R.; Hall, M.; Kallos, G.; Martin, S.; Roeck, J.; Ryder, J.; Smith, P. *Macromolecules* **1986**, *19*, 2466–2470. (d) Tomalia, D. A.; Naylor, A. M.; Goddart, W. A. *Angew. Chem., Int. Ed.* **1990**, *29*, 138–175. (e) Sherf, U.; Müllen, K. *Synthesis* **1992**, 1–2. (f) Tomalia, D. A.; Durst, H. D. *Top. Curr. Chem.* **1993**, *165*, 193–313. (g) van der Made, A. W.; van Leeuwen, P. W. N. M.; de Wilde, J. C.; Brandes, R. A. C. *Adv. Mater.* **1993**, *5*, 466–468. (h) Zhou, L. L.; Roovers, J. *Macromolecules* **1993**, *26*, 963–968. (i) Sournies, F.; Crasnier, F.; Graffeuil, M.; Faucher, J.-P.; Lahana, R.; Labarre, J.-F. *Angew. Chem., Int. Ed.* **1995**, *34*, 578–581. (j) Devadoss, C.; Bharathi, P.; Moore, J. S. *J. Am. Chem. Soc.* **1996**, *118*, 9635–9644. (k) Moore, J. S. *Acc. Chem. Res.* **1997**, *30*, 402–413. (l) Caminade, A. M.; Majoral, J. P. In *Dendrimers*; Vögtle, F., Ed.; Topics in Current Chemistry; Springer: Berlin, 1998; Vol. 170, pp 79−124. (m) Berresheim, A. J.; Müller, M.; Müllen, K. *Chem. Rev.* **1999**, *99*, 1747–1785. (n) Watson, M. D.; Fechtenkotter, A.; Müllen, K. *Chem. Rev.* **2001**, *101*, 1267–1300. (o) Ihre, H.; Padilla de Jesús, O. L.; Fréchet, J. M. J. *J. Am. Chem. Soc.* **2001**, *123*, 5908–5917. (p) Dvornic, P. R.; Li, J.; de Leuze-Jallouli, A. M.; Reeves, S. D.; Owen, M. J. *Macromolecules* **2002**, *35*, 9323. (q) Dvornic, P. R. *J. Polym. Sci., Part A* **2006**, *44*, 2755–2773. (r) Furuta, P.; Brooks, J.; Thompson, M. E.; Fréchet, J. M. J. *J. Am. Chem. Soc.* **2006**, *125*, 13165–13172.

Scheme 2. Synthesis of the G_1-27-Allyl Dendrimer[9a]

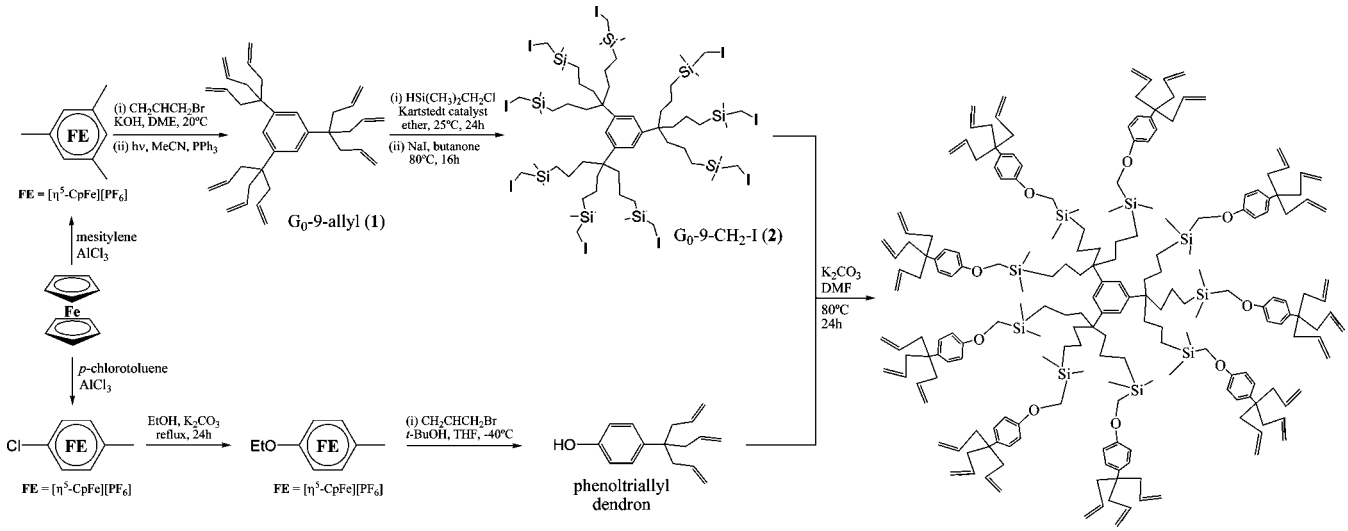

[a] This dendritic construction was continued, using the phenoltriallyl dendron as a building block, until G_7 to synthesize the precursors of the ferrocenyl and pentamethylferrocenyl dendrimers (see eqs 1−7).

Scheme 3. Synthesis of the Ferrocenyl Derivative **14**

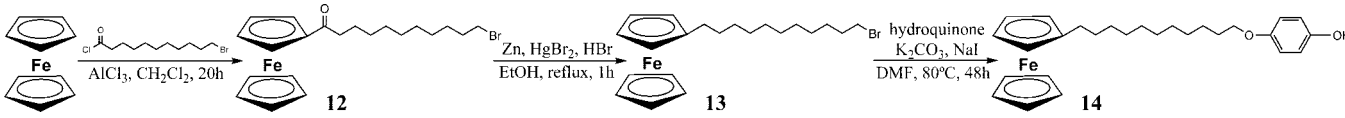

redox active termini, i.e. ferrocenyl (Fc) and pentamethylferrocenyl (Fc*) were used to functionalize the organic dendrimers. Knowing that these metallocenes present fully reversible redox properties in the monomer form, their introduction into the dendrimers will extend their redox chemistry to the nanoscale.

The strategy of lengthening the branches was used in order to achieve the functionalization of the giant dendrimers[9] with these metallocenes, because of the forecasted bulk problem. Phenolic derivatives of ferrocene and pentamethylferrocene possessing a "long tether" were synthesized, in order to attach them to the dendrimers using the Williamson reaction (which has already been shown to be an efficient reaction to construct and functionalize dendrimers[9]). The polyferrocenyl dendrimers were synthesized for eight generations, from G_0 (with nine termini) to G_7 (with a theoretical total number of termini, TNT, of 19 683) and pentamethylferrocenyl dendrimers were synthesized for G_0 (nine termini) and G_7 (19 683 termini).

2.1. Ferrocenyl Dendrimers Series (Fc). The synthesis of a phenolic derivative of ferrocene containing a long alkyl chain was achieved by Friedel-Craft reaction between 11-bromoundecanoyl chloride and ferrocene in the presence of $AlCl_3$, yielding the 11-bromoundecanoyl ferrocene **12**, followed by Clemmensen reduction of the ketone group, yielding the 11-bromoundecyl ferrocene **13**.[15] Williamson reaction between **13** and hydroquinone afforded the phenolic derivative **14** (Scheme 3).

The ferrocenyl dendrimers were synthesized by Williamson reaction between the iodomethyl dendrimers and **14** using an excess of K_2CO_3, in DMF, at 80 °C, for 48 h. Eight different generations (from G_0 with nine branches to G_7 with a TNT of 19 683) were synthesized in order to study their physical properties with the increasing number of generations (eqs 1−8). All the ferrocenyl dendrimers were characterized by ^1H, ^{13}C, and ^{29}Si NMR, elemental analysis, UV−vis. spectroscopy,

(9) (a) Sartor, V.; Djakovitch, L.; Fillaut, J.-L.; Moulines, F.; Neveu, F.; Marvaud, V; Guittard, J.; Blais, J.-C.; Astruc, D. *J. Am. Chem. Soc.* **1999**, *121*, 2929–2930. (b) Ruiz, J.; Lafuente, G.; Marcen, S.; Ornelas, C.; Lazare, S.; Blais, J.-C.; Cloutet, E.; Astruc, D. *J. Am. Chem. Soc.* **2003**, *125*, 7250–7257.

(10) (a) Newkome, G. R.; Yao, Z.; Baker, G. R.; Gupta, V. K. *J. Org. Chem.* **1985**, *50*, 2003. (b) Newkome, G. R.; Moorefield, C. N.; Baker, G. R. *Aldrichim. Acta* **1992**, *25* (N°2), 21. (c) Lescanec, R. L.; Muthukumar, M. *Macromolecules* **1990**, *23*, 2280–2288. (d) Mansfield, M. L.; Klushin, L. I. *Macromolecules* **1993**, *26*, 4262–4268. (e) Boris, D.; Rubinstein, M. *Macromolecules* **1996**, *29*, 7251–7260. (f) Naidoo, K. J.; Hughes, S. J.; Moss, J. R. *Macromolecules* **1999**, *32*, 331–341.

(11) See refs 1, 6, 7 and (a) Takada, K.; Diaz, D.; Abruña, H.; Cuadrado, I.; Casado, C. M.; Alonso, B.; Lobete, F.; Garcia, B.; Losada, J. *J. Am. Chem. Soc.* **1997**, *119*, 10763–10770. (b) Shu, C.-F.; Shen, H. M. *J. Mater. Chem.* **1997**, *7*, 47. (c) Tokuhisa, H.; Zhao, M.; Baker, L. A.; Phan, V. T.; Dermody, D. L.; Garcia, M. E.; Peez, R. F.; Crooks, R. M.; Mayer, T. M. *J. Am. Chem. Soc.* **1998**, *120*, 4492. (d) Schneider, R.; Köllner, C.; Weber, I.; Togni, A. *Chem. Commun.* **1999**, 2415–2416. (e) Casado, C. M.; Alonso, B.; Morán, M.; Cuadrado, I.; Losada, J. *J. Electroanal. Chem.* **1999**, *463*, 87–93. (f) Turin, C. O.; Chiffre, J.; de Montauzon, D.; Daran, J.-C.; Caminade, A.-M.; Manoury, E.; Balavoine, G.; Majoral, J.-P. *Macromolecules* **2000**, *33*, 7328–7336. (g) Casado, C. M.; Gonzales, B.; Cuadrado, I.; Alonso, B.; Morán, M.; Losada, J. *Angew. Chem., Int. Ed.* **2000**, *39*, 2135–2138. (h) Gonzales, B.; Cuadrado, I.; Casado, C. M.; Alonso, B.; Pastor, C. *Organometallics* **2000**, *120*, 4023–4029. (i) Alonso, B.; Casado, C. M.; Cuadrado, I.; Moran, M.; Kaifer, A. E. *Chem. Commun.* **2002**, *16*, 1778–1779. (j) Brettar, J.; Burgi, T.; Donnio, B.; Guillon, D.; Klappert, R.; Sharf, T.; Descheneau, R. *Adv. Funct. Mater.* **2006**, *16*, 260–267. (k) Kaifer, A. E. *Eur. J. Inorg. Chem.* **2007**, 5015–5027.

(12) (a) Meyer, W. H. *Adv. Mater.* **1998**, *6*, 439–448. (b) Romero, P. G.; Torres-Gómez, G. *Adv. Mater.* **2000**, *19*, 1454–1456. (c) Stanish, I.; Lowy, D. A.; Hung, C. W.; Singh, A. *Adv. Mater.* **2005**, *9*, 1194–1198. (d) Song, H.-K.; Palmore, G. T. R. *Adv. Mater.* **2006**, *13*, 1764–1768. (e) Jeon, N. L.; Clem, P.; Jung, D. Y.; Lin, W.; Girolami, G. S.; Payne, D. A.; Nuzzo, R. G. *Adv. Mater.* **1997**, *11*, 891–895. (f) Oldfield, G.; Ung, T.; Mulvaney, P. *Adv. Mater.* **2000**, *20*, 1519–1522. (g) Lidgi-Guigui, N.; Dablemont, C.; Veautier, D.; Viau, G.; Seneor, P.; van Dau, F. N.; Mangeney, C.; Vaurès, A.; Deranlot, C.; Friederich, A. *Adv. Mater.* **2007**, *13*, 1729–1733.

Scheme 4. Synthesis of the Pentamethylferrocenyl Derivative Containing a Long Alkyl Chain and a Phenol Termini.

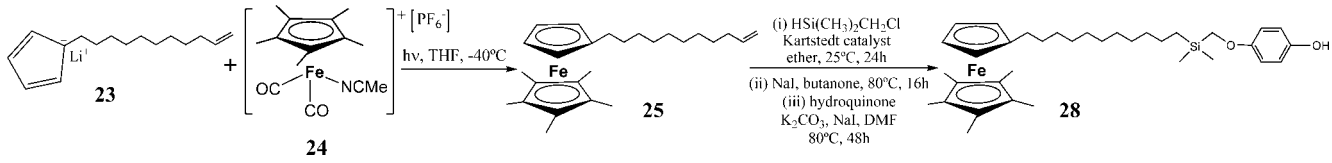

dynamic light scattering (DLS), atomic force microscopy (AFM), cyclic voltammetry (CV) and coulometry. The two first generations (G_0-Fc and G_1-Fc) show the corresponding molecular peaks at 5 167.50 (calcd. for $C_{306}H_{444}O_{18}Si_9Fe_9$, 5 166.27) and 17 241.55 (calcd for $C_{1017}H_{1488}O_{63}Si_{36}Fe_{27}$, 17 241.55) in the MALDI-TOF mass spectra, confirming the structure of the polyferrocenyl dendrimers (see the Supporting Information, pages SI10 and SI13). The analytical data confirm the structures up to G_5, but above this generation (G_6 and especially G_7) the carbon analysis that is found is low because of structural defects and increased ability to encapsulate external impurities (solvents, water, inorganic salts).

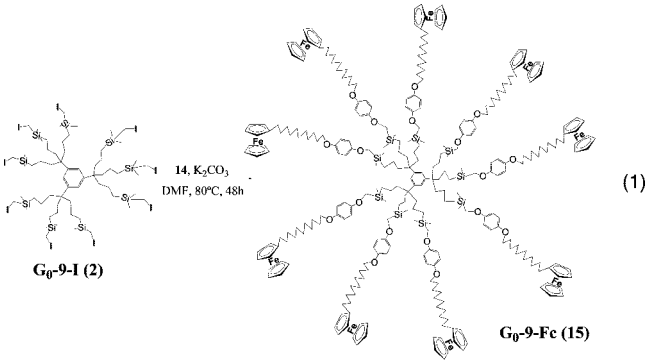

(1)

$$G_1\text{-}27\text{-}CH_2I \xrightarrow[\text{DMF, 80°C, 48h}]{\mathbf{14},\ K_2CO_3} G_1\text{-}27\text{-}Fc \quad (2)$$
(3) (16)

$$G_2\text{-}81\text{-}CH_2I \xrightarrow[\text{DMF, 80°C, 48h}]{\mathbf{14},\ K_2CO_3} G_2\text{-}81\text{-}Fc \quad (3)$$
(4) (17)

$$G_3\text{-}243\text{-}CH_2I \xrightarrow[\text{DMF, 80°C, 48h}]{\mathbf{14},\ K_2CO_3} G_3\text{-}243\text{-}Fc \quad (4)$$
(5) (18)

$$G_4\text{-}729\text{-}CH_2I \xrightarrow[\text{DMF, 80°C, 48h}]{\mathbf{14},\ K_2CO_3} G_4\text{-}729\text{-}Fc \quad (5)$$
(6) (19)

$$G_5\text{-}2187\text{-}CH_2I \xrightarrow[\text{DMF, 80°C, 48h}]{\mathbf{14},\ K_2CO_3} G_5\text{-}2187\text{-}Fc \quad (6)$$
(7) (20)

$$G_6\text{-}6561\text{-}CH_2I \xrightarrow[\text{DMF, 80°C, 48h}]{\mathbf{14},\ K_2CO_3} G_5\text{-}6561\text{-}Fc \quad (7)$$
(8) (21)

$$G_7\text{-}19683\text{-}CH_2I \xrightarrow[\text{DMF, 80°C, 48h}]{\mathbf{14},\ K_2CO_3} G_7\text{-}19683\text{-}Fc \quad (8)$$
(9) (22)

2.2. Pentamethylferrocenyl Dendrimers Series (Fc*). To synthesize a phenolic derivative of pentamethylferrocene, we first functionalized cyclopentadiene with a long alkyl chain and an olefin termini (**23**) by reaction of sodium cyclopentadienyl with 11-bromo-1-undecene. This cyclopentadienyl derivative **23** was then used in a ligand substitution reaction in the complex $[Cp^*Fe(CO)_2(NCMe)][PF_6]$ (**24**), induced by UV light at −40 °C, affording the functionalized pentamethylferrocene **25**. Indeed, previous photocleavage studies of cationic $[CpFeL_3]^+$ and $[Cp^*FeL_3]^+$ (L_3 = arene or 3 CO's) derivatives in the presence of substituted cyclopentadienyl derivatives have been shown to provide a method of choice to synthesize ferrocenes containing two different rings.[13] Hydrosilylation of **25** with chloromethyl(dimethyl)silane in the presence of the Kartstedt catalyst yielded compound **26**. Subsequent to the substitution of chloride by iodide in compound **26**, Williamson reaction with hydroquinone afforded the phenolic derivative **28** (Scheme 4).

The pentamethylferrocenyl dendrimers were synthesized by Williamson reaction between the iodomethyl-terminated dendrimers and **28** using excess of K_2CO_3 in DMF at 80 °C for 48 h. The reaction was carried out for G_0 and G_7 (eqs 10 and 10), and the products were characterized by ^1H, ^{13}C and ^{29}Si NMR, elemental analysis, UV−vis spectroscopy, dynamic light scattering, and cyclic voltammetry. G_0-Fc* shows in the MALDI-TOF mass spectra the corresponding molecular peak at 6 450.30 (calcd for $C_{378}H_{606}O_{18}Si_{18}Fe_9$, 6647.12) confirming the expected structure (see the Supporting Information, page SI31).

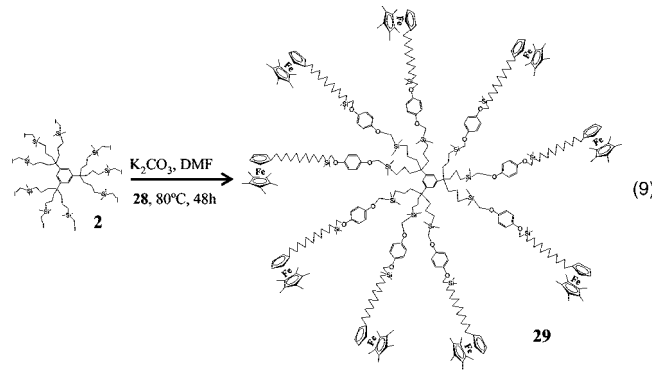

(9)

$$G_7\text{-}19683\text{-}CH_2I \xrightarrow[\mathbf{28},\ 80°C,\ 48h]{K_2CO_3,\ DMF} G_7\text{-}19683\text{-}Fc^* \quad (10)$$
(9) (30)

3. Characterization of the Metallodendrimers. 3.1. UV−Vis Spectroscopy. In order to estimate the number of defects in the dendritic structures due to the divergent synthesis, we investigated the UV−vis spectroscopy of the dendrimers. The Lambert−Beer law ($A = \varepsilon lc$) was used to determine the actual total number of metallocene groups in the dendrimers.[18]

The UV−vis spectra of the metallocenes present an absorption band at 440 nm in the Fc series, and at 423 nm in the Fc* series. The number of metallocene termini in each dendrimer can be estimated by comparing the molar extinction coefficient ε of

(13) (a) Gill, T. P.; Mann, K. R. *Inorg. Chem.* **1983**, *22*, 1986–1988. (b) Catheline, D.; Astruc, D. *J. Organomet. Chem.* **1983**, *248*, C9–C12. (c) Catheline, D.; Astruc, D. *J. Organomet. Chem.* **1984**, *266*, C11–C14. (d) Catheline, D.; Astruc, D. *Organometallics* **1984**, *3*, 1094–1100. (e) McNair, A. M.; Schrenck, J. L.; Mann, K. R. *Inorg. Chem.* **1984**, *23*, 633–636. (f) Schrenk, J. L.; McNair, A. M.; McCormick, F. B.; Mann, K. R. *Inorg. Chem.* **1986**, *25*, 3504–3508. (g) Ruiz, J.; Astruc, D. *Inorg. Chim. Acta* **2008**, *361*, 1–4.

(14) (a) Koppel, D. E. *J. Chem. Phys.* **1972**, *57*, 4814–4820. (b) Frisken, B. *J. Appl. Opt.* **2001**, *40*, 4087–4091. (c) Hassan, P. A.; Kulshreshtha, S. K. J. *Colloid Interface Sci.* **2006**, *300*, 744–748.

Table 1. Number of Termini Calculated of the Metallocene-Terminated Dendrimers Using the Lambert−Beer Law and Coulometry Results

series	product	λ (nm)	theoretical no. of termini	ε	calcd no. of termini[a]	electrolysis[b] (%)
Fc	monomer **14**	440	1	$\varepsilon_0 = 116$		
	G_0-Fc (**15**)	440	9	1064	9 ± 1	98
	G_1-Fc (**16**)	440	27	3096	27 ± 1	99
	G_2-Fc (**17**)	440	81	9417	81 ± 4	95
	G_3-Fc (**18**)	440	243	24 808	210 ± 10	94
	G_4-Fc (**19**)	440	729	81 709	700 ± 40	90
	G_5-Fc (**20**)	440	2 187	231 678	$2\,000 \pm 100$	92
	G_6-Fc (**21**)	440	6 561	724 728	$6\,200 \pm 300$	88
	G_7-Fc (**22**)	440	19 683	1 629 242	$14\,000 \pm 1000$	83
Fc*	monomer **28**	423	1	$\varepsilon_0 = 148$		
	G_0-Fc* (**29**)	423	9	1364	9 ± 1	
	G_7-Fc* (**30**)	423	19 683	2 100 122	$14\,000 \pm 1000$	

[a] $\varepsilon/\varepsilon_0$: represents the experimental branch number calculated from Lambert−Beer law. [b] The data are provided with an estimated error of ±2%.

the dendrimers with that of the corresponding monomer (ε_0). The linearity of the absorption with the number of ferrocenyl groups in the low-generation dendrimers confirms that there is no interaction between the ferrocenyl groups that would perturb the validity of the Lambert−Beer law. Thus, the number of termini calculated using the Lambert−Beer law confirms the existence of the defects in the dendritic structures that is marked for the high generations (Table 1). More specifically, these defects are relatively not very numerous until generation 5, but their number becomes higher when the generations 6 and 7 are reached. The structural defects follow the same tendency, presenting similar results independently of the nature of the peripheral redox group (for example, G_7-Fc and G_7-Fc* both present an experimental number of termini of $14\,000 \pm 1000$). The comparison of the three last generations of ferrocenyl dendrimers in Figure 1 at the same concentration of dendrimer shows the progression of the number of ferrocenyl termini from each generation to the next.

3.2. Cyclic Voltammetry. All the cyclic voltammograms of the metallodendrimers present a single reversible redox wave at the same potential as that of the corresponding metallocene (Figure 2).[6,7] The single wave can be explained by the weak electrostatic factor in dendrimers, the redox centers being very far from one another. The electrochemical reversibility observed for all the generations shows that the electron-hopping mechanism among the redox centers of the periphery is extremely efficient. Thus, electron transfer is fast between all the redox groups of the dendrimers and the electrode, subsequent to electron transfer at the optimum distance among the flexible peripheral redox centers. A precise analysis of this later type

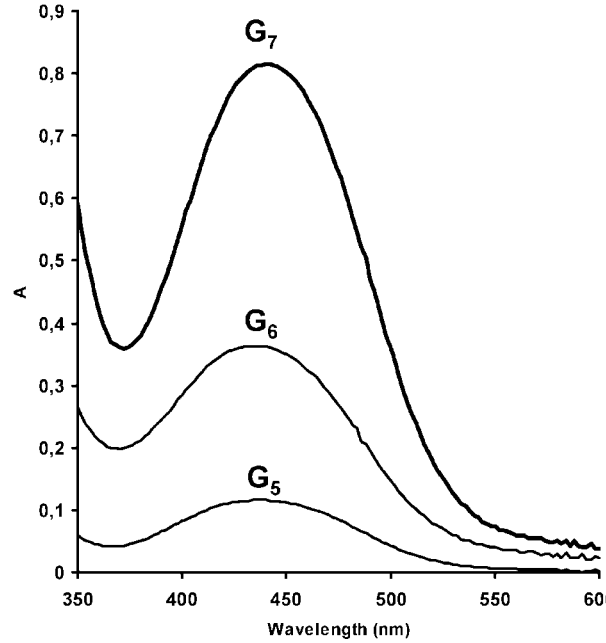

Figure 1. UV−vis spectra of G_5, G_6, and G_7 of ferrocenyl dendrimers at 5×10^{-7} M in dichloromethane.

of mechanism in metallodendrimers has been proposed by Amatore et al. for dendrimers containg 64 peripheral branches terminated by $[Ru(terpy)_2]^{2+}$. It is based on the measured electron hopping rate constant using ultramicroelectrodes and on a Smoluchowski-type model developed to take into account viscosity effects during the displacement of the Ru(III)/Ru(II)$(tpy)_2$ redox centers around their equilibrium positions.[16a,b] This analysis involves very fast scan rates, thus the events proposed by Amatore et al. have time to proceed within the time scale of the present studies.

In addition to electron hopping through space, the dendrimers rotate fast within the electrochemical time scale, so that all the redox groups come close to the electrode within this time scale.[6,7] Fast rotation alone can explain the fast heterogeneous electron transfer with the small dendrimers. For the high generations, however, the hopping mechanism between nearby centers appears to be much easier than the fast-rotation mechanism. In favor of this explanation, it is noteworthy that with derivatized electrodes with the high-generation dendrimers, complete rotation is no longer possible, but electron transfer is still fast.

The ferrocenyl dendrimers present a single redox wave at 490 mV vs $FeCp^*_2$ in dichloromethane (electrolyte,

(15) Saji, T.; Hoshino, K.; Ishii, Y.; Goto, M. *J. Am. Chem. Soc.* **1991**, *113*, 450–456.
(16) (a) Amatore, C.; Grun, F.; Maisonhaute, E. *Angew. Chem., Int. Ed.* **2003**, *40*, 4944–4947. (b) Amatore, C.; Bouret, Y.; Maisonhaute, E.; Goldsmith, J. I.; Abruña, H. D. *Chem.—Eur. J.* **2001**, *7*, 2206–2226. (c) For electrochemical redox recognition with ferrocene systems, see: Beer, P. D.; Gale, P. A. *Angew. Chem., Int. Ed.* **2001**, *40*, 486–506.
(17) For the first observation of the flattening of dendrimers on a surface, see: (a) Hierlemann, A.; Campbell, J. K.; Baker, L. A.; Crooks, R. M.; Rico, A. J. *J. Am. Chem. Soc.* **1998**, *120*, 5323–5324, see also. (b) Li, J.; Piehler, L. T.; Qin, D., Jr.; Tomalia, D. A. *Langmuir* **2000**, *16*, 5613–5617. (c) Zhang, H.; Grim, P. C. M.; Vosch, T.; Wiesler, U.-M.; Berresheim, A. J.; Mullen, K.; De Schryver, F. C. *Langmuir* **2000**, *16*, 9294–9298. (d) Coen, M. C.; Lorenz, K.; Kressler, J.; Frey, H.; Mulhaupt, R. *Macromolecules* **2000**, *29*, 8069–8079. (e) Mecke, A.; Lee, I.; Baker, J. R., Jr.; Holl, M. M. B.; Orr, B. G. *Eur. Phys. J. E* **2004**, *14*, 7–10.
(18) (a) Cheon, K.-S.; Kazmaier, P. M.; Keum, S.-R.; Park, K.-T.; Buncel, E. *Can. J. Chem.* **2004**, 551–556. (b) Liu, D.; De Feyter, S.; Cotlet, M.; Stefan, A.; Wiesler, U.-M.; Herrman, A.; Grebel-Koehler, D.; Qu, J.; Müllen, K.; De Schryver, F. C. *Macromolecules* **2003**, *16*, 5918–5928.

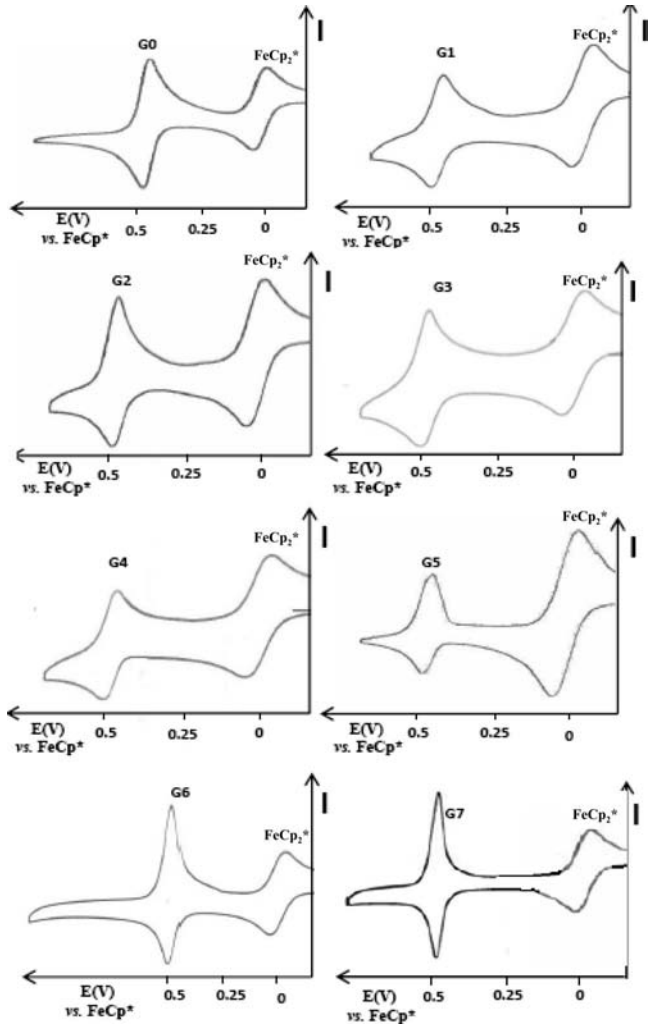

Figure 2. Cyclic voltammograms obtained for the eight generations from G_0-Fc to G_7-Fc using decamethylferrocene ($FeCp^*_2$) as an internal reference (solvent, dichloromethane; electrolyte, [*n*-Bu_4N][PF_6] 0.1 M; scan rate, 200 mV s^{-1}; 20 °C; working and counter electrodes, Pt; quasi-reference electrode, Ag).

[*n*-Bu_4N][PF_6] 0.1 M; scan rate, 200 mV s^{-1}; 20 °C; working and counter electrodes, Pt; quasi-reference electrode, Ag). The number of electrons involved in each redox process was calculated using the Bard−Anson equation:[19a,b] for G_0 (9 ferrocenyl termini), G_1 (27 ferrocenyl termini), and G_2 (81 ferrocenyl termini), the numbers 9, 27, and 103 electrons were found, respectively. After G_2, this kind of calculation is marred by the adsorption of the ferrocenyl dendrimers onto the electrode surface (for example: for G_3 with 243 ferrocenyl termini and G_6 with 6561 ferrocenyl termini, numbers obtained are 700 and 30000 electrons respectively using the Bard−Anson equation). The adsorption phenomenon becomes all the more important as the generation is higher, and this can be evidenced by the difference between the anodic and cathodic potential that becomes lower (<60 mV) and lower as the generation number increases (Figure 2). This pronounced adsorption of large ferrocenyl dendrimers leads to the facile formation of derivatized electrodes[19c−e] with such redox dendrimers upon dipping the electrode into the solution of dendrimer and scanning a few times around the region of the ferrocenyl redox potential. These modified electrodes are actually very robust, and washing with dichloromethane does not remove the dendrimer. Moreover, recognition of ATP^{2-} is possible as its *n*-Bu_4N^+ salt, even

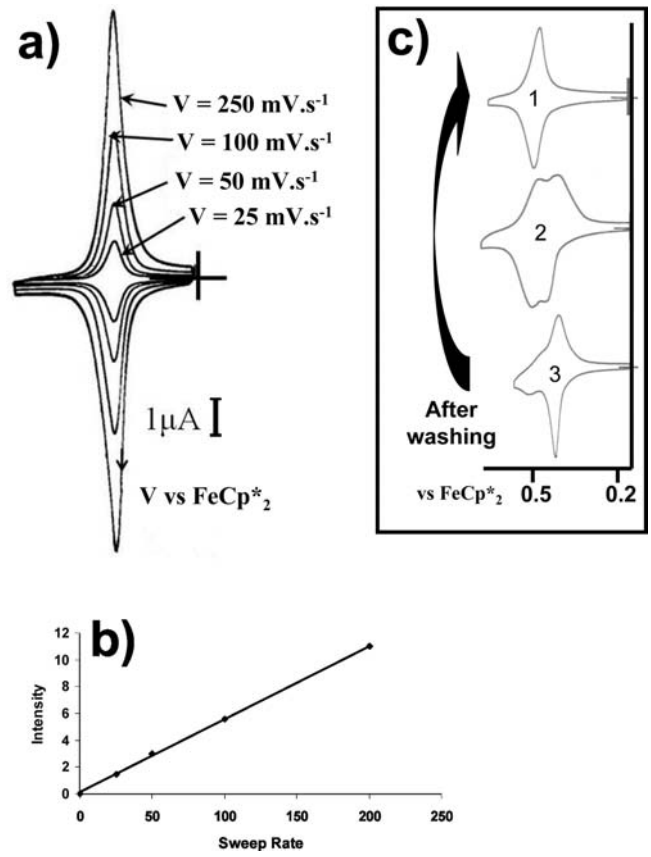

Figure 3. (a) Modified Pt electrode with G_7-Fc; (b) linearity of the intensity/sweep rate function; (c) ATP^{2-} sensing, and regeneration of the modified electrode for reuse.

though there is no interaction site near the ferrocenyl group on the dendrimer tethers to perturb the ferrocenyl group and modify its redox potential.[16c] Indeed, the electrostatic interaction between the multiply charged ferrocenium dendrimer and ATP^{2-} is large and sufficient by itself to significantly perturb the redox system and decrease the ferrocenyl potential as can be seen in Figure 3. After the experiment, [ATP][*n*-$Bu_4N]_2$ can be washed, and the modified electrode can be used for another experiment.

The cyclic voltammogramms of the pentamethylferrocenyl dendrimers were also recorded in dichloromethane, and they were shown to present a single redox wave at 210 mV vs $FeCp^*_2$ (electrolyte, [*n*-Bu_4N][PF_6] 0.1 M; scan rate, 200 mV s^{-1}; 20 °C; working and counter electrodes, Pt; quasi-reference electrode, Ag). Also in this case, the number of electrons could be calculated for G_0-Fc* (9) but for G_7-Fc* the absorption phenomenon induces erroneous values using the Bard−Anson equation.

3.3. Coulometry. Whereas the number of electrons for metallodendrimers could not be calculated for the higher generations due to the absorption phenomenon, the ferrocenyl metallodendrimers were also characterized by coulometry for all the generations, and the data provided satisfactory results in terms of numbers of metallocene redox units in the dendrimers. The total current Q ($Q = nFN$) used to oxidize the dendrimers can be compared with the calculated one (one electron per ferrocene). The results found for the electrolysis of the two first generations fit to the theoretical redox group number (98 and 99%), and they are higher than 90% until G_5, showing the rather good correspondence between the actual redox group numbers and the theoretical ones. For the last generation (G_7), the

Table 2. Hydrodynamic Diameters Obtained by DLS and Calculated Diffusion Coefficients and Volumes of the Metallodendrimers

series	product[a]	theoretical MW (g mol^{-1})	estimated MW[b] (g mol^{-1})	hydrodynamic diameter[c] (nm)	diffusion coefficient[d] (m^2 s^{-1})	volume[e] (m^3)	density[f](Kg/m^3)
Fc	G_2-Fc (**17**)	53 468	$(5.2 \pm 0.14) \times 10^4$	11.1 ± 0.8	8.76×10^{-14}	$(7.2 \pm 1.4) \times 10^{-25}$	$(1.2 \pm 0.1) \times 10^2$
	G_3-Fc (**18**)	162 146	$(1.54 \pm 0.08) \times 10^5$	16.6 ± 0.5	6.57×10^{-14}	$(1.70 \pm 0.15) \times 10^{-24}$	$(1.5 \pm 0.2) \times 10^2$
	G_4-Fc (**19**)	488 181	$(4.60 \pm 0.3) \times 10^5$	20.5 ± 0.4	4.63×10^{-14}	$(4.5 \pm 0.2) \times 10^{-24}$	$(1.7 \pm 0.2) \times 10^2$
	G_5-Fc (**20**)	1 466 316	$(1.35 \pm 0.1) \times 10^6$	24.3 ± 0.5	3.89×10^{-14}	$(7.5 \pm 0.4) \times 10^{-24}$	$(3.0 \pm 0.3) \times 10^2$
	G_6-Fc (**21**)	4 400 608	$(4.0 \pm 0.4) \times 10^6$	27.6 ± 0.5	3.52×10^{-14}	$(1.10 \pm 0.10) \times 10^{-23}$	$(6.0 \pm 0.6) \times 10^2$
	G_7-Fc (**22**)	13 203 566	$(1.0 \pm 0.2) \times 10^7$	29.5 ± 1.1	3.29×10^{-14}	$(1.34 \pm 0.20) \times 10^{-23}$	$(1.2 \pm 0.2) \times 10^3$
Fc*	G_7-Fc* (**30**)	16 005 053	$(1.2 \pm 0.3) \times 10^7$	30.0 ± 1.4	3.24×10^{-14}	$(1.41 \pm 0.20) \times 10^{-23}$	$(1.4 \pm 0.2) \times 10^3$

[a] It was not possible to obtain the hydrodynamic diameter of dendrimers of G_0 and G_1 by DLS, because their size is below the limit for this technique. [b] Molecular weight calculated taking into account the defects estimated by UV−vis. and coulometry (2.5% for G_2, 5% for G_3, 6% for G_4, 8% for G_5, 10% for G_6,and 23% for G_7). [c] Measured at 25 °C in dichloromethane; the hydrodynamic diameter value was obtained from statistical CONTIN analysis with 2% error for G_4, G_5, and G_6; the error is larger for the low generations, because their size is at or near the low limit for this technique, and for G_7, which contains many defects. [d] Calculated using the Stokes−Einstein equation. [e] Considering the globular dendrimer shape as a perfect sphere ($V = (4/3)\pi r^3$). [f] The density was calculated taking into account the average MW calculated by UV−vis and coulometry.

Table 3. Average Height Obtained by AFM on a Mica Surface for Each Generation G_n of Ferrocenyl Dendrimers G_n-Fc.

dendrimer	no. of branches	height (nm)
G_0-Fc (**15**)	9	0.8 ± 0.1
G_1-Fc (**16**)	27	1.5 ± 0.2
G_2-Fc (**17**)	81	2.5 ± 0.2
G_3-Fc (**18**)	243	3.0 ± 0.3
G_4-Fc (**19**)	729	3.5 ± 0.3
G_5-Fc (**20**)	2187	4.5 ± 0.4
G_6-Fc (**21**)	6561	6.0 ± 0.6
G_7-Fc (**22**)	19 683	7.5 ± 1.5

electrolysis shows a difference of 17% between the theoretical number of electrons and the obtained one. The results obtained for the coulometry of the ferrocenyl dendrimers series are gathered in Table 1.

3.4. Dynamic Light Scattering (DLS). Dynamic light scattering (DLS)[14] is a useful technique to characterize the metallodendrimers, allowing to determine, or to estimate, the size (hydrodynamic diameter) of the dendrimers in solution and consequently their diffusion coefficient (D) using the Stokes−Einstein equation: $D = kT/6\pi\eta R_h$, where the R_h is the hydrodynamic radius, η is the solvent viscosity, k is the Boltzmann constant, and T is the temperature. All the values of the hydrodynamic diameter reported in Table 2 were found to be constant for three different concentrations. These hydrodynamic diameter values in this way usually overestimate the true dendrimer diameter, because (i) the solvation sphere is included in this hydrodynamic value, (ii) for the small dendrimers, the DSL technique is not applicable, and (iii) for average generations such as G_2, the dendrimers are not fully spherical, and the technique reaches its limit. The progression of the observed values when the generation increases clearly shows the size progression, however.

It is known that dendrimers present globular shapes,[1] and they are usually considered as perfect spheres in order to calculate their physical properties. We also used this approximation to estimate, the volume and the density of the metallodendrimers (Table 2). The difference between theoretical and actual values becomes significant for G_6 and especially G_7 that present many defects and whose molecular masses are much reduced compared to the theoretical ones. There is no significant difference in the diameter for both neutral series, as expected, i.e., G_7-Fc has an observed diameter of 29.5 ± 1.1 nm and G_7-Fc* has an observed diameter of 30.0 ± 1.4 nm.

In these series of dendrimers, the number of branches is multiplied by three at each generation and, according to Figure 4a, this increase perfectly fits the exponential function (with R

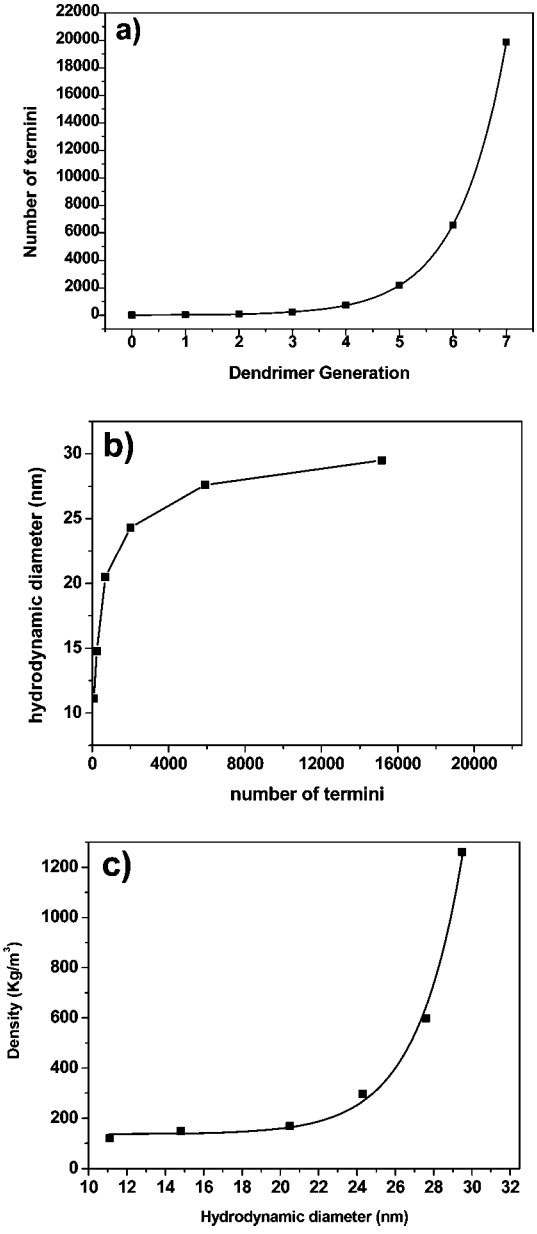

Figure 4. Relationship between the (a) number of termini vs the generation of dendrimer: $y = 5.15 + 8.56e^{(x/0.903)}$, ($R = 1.00$); (b) number of termini vs the hydrodynamic diameter; (c) the hydrodynamic diameter vs the density of the dendrimer: $y = 136 + 0.00619e^{(x/2.44)}$, ($R = 0.996$).

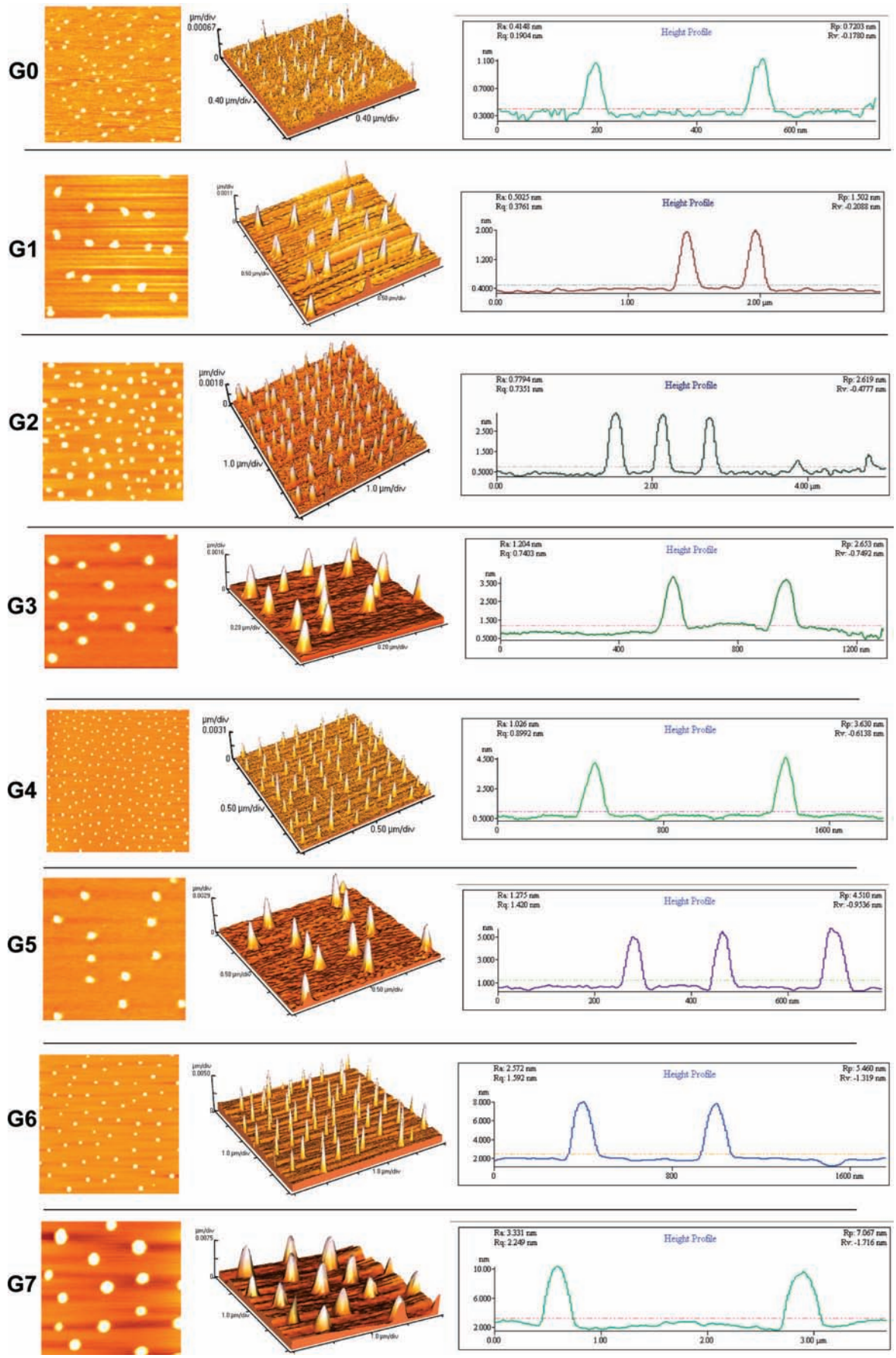

Figure 5. AFM images obtained for the ferrocenyl dendrimers (G_n-Fc).

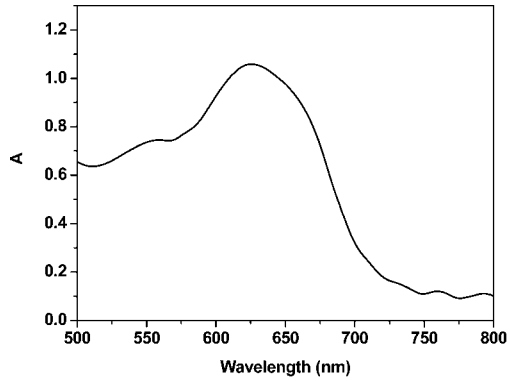

Figure 6. UV−vis spectra of the oxidized G_0-Fc in dichloromethane.

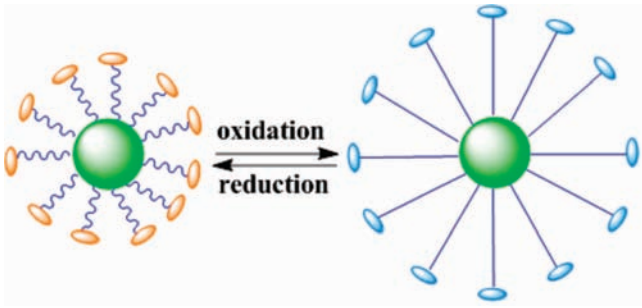

Figure 7. Representation of the "breathing mechanism" of the giant metallodendrimers upon redox switching between the neutral orange form and the cationic blue form.

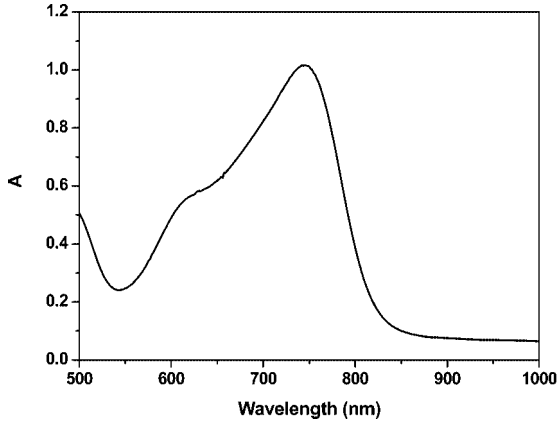

Figure 8. UV−vis spectrum of the oxidized G_0-Fc* in dichloromethane.

= 1). The DLS data show that the hydrodynamic diameter increases almost linearly with the number of termini until G_5 (2187 branches). For the next generations, the increase of the diameter seems to be less significant (Figure 4b), but the accuracy of the technique is not sufficient for a conclusion concerning this point. Figure 4c shows that the density increases exponentially with the increase of the number of termini.

3.5. Atomic Force Microscopy (AFM). For the design of nanodevices with optimal properties, it is essential to study the structure and the behavior of dendrimers in the condensed state in contact with surfaces subsequent to evaporation of the solvent. Flat substrates such as mica have already been shown to be useful models for this kind of interaction.[17] Mica possesses a negative surface charge density and is readily accessible to high-resolution scanning probe techniques.[17] Previous studies, using AFM experiments, have already demonstrated that dendrimers

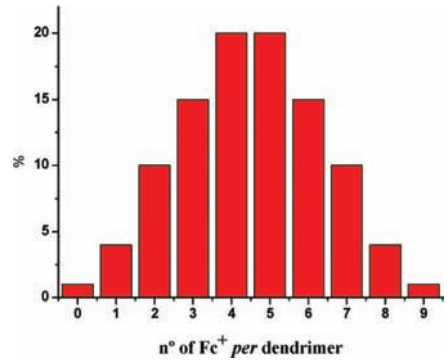

Figure 9. Statistical distribution of the Fe^{II} and Fe^{III} species on the mixed-valence dendrimers. For instance, with G_0 (9 terminal branches) the statistical distribution obtained with a simple binomial law gives 24.6% of $4Fe^{II}$-$5Fe^{III}$, 16.4% $3Fe^{II}$-$6Fe^{III}$, 7% $2Fe^{II}$-$7Fe^{III}$, 1.7% $1Fe^{II}$-$8Fe^{III}$, and 0.2% $0Fe^{II}$-$9Fe^{III}$, etc.

are extensively deformed from their globular shape when they are neat, in contact with a surface presenting a flat disk.[17] In this work, AFM was used to study the behavior of the giant ferrocenyl dendrimers on a mica surface. An ether solution of the dendrimer was deposited on a mica surface, and the solvent was evaporated before AFM observation. In spite of the flattening of the dendrimers on a mica surface, it is possible to observe a progression of the dendrimer size upon increasing the generation number (Table 3). The height of dendrimers in each generation was quite uniform in the monolayers, as can be observed in Figure 5. Interestingly, the width of each AFM spot is relatively regular suggesting agglomeration of the metallodendrimers among one another and also the discrete limits of this agglomeration (as for metallic nanoparticles) that is rather regular from a dendrimer particle to the next. In other words, on mica surface, the dendrimers behave like atoms in forming relatively monodisperse nanoparticles. This feature looks quite general, and is best observed for the dendrimers below G_7-Fc.

4. Chemical Oxidation of the Fc and Fc* Series. The ferrocenyl and pentamethylferrocenyl dendrimers were chemically oxidized and isolated and the dendritic polycations were reduced, in order to confirm by NMR their redox stability after a complete oxidoreduction cycle.

The ferrocenyl dendrimers were oxidized using a stoichiometric amount of acetylferrocenium tetrafluoroborate [Fc-COMe][BF_4],[20] in dry dichloromethane at room temperature for 5 min. After the oxidized dendrimers were washed with ether in order to remove the acetylferrocene formed, they were isolated as blue solids and characterized by UV−vis spectroscopy, showing an absorption band at 624 nm (Figure 6). The reduction of the ferrocenium dendrimers was carried out with an aqueous solution of $TiCl_3$. The ferrocenyl dendrimers series was thus shown to be highly stable in both the oxidized ferrocenium and reduced ferrocene forms by quantitative interconversion, their structure being confirmed by ^{1}H NMR after a complete oxido-reduction cycle.

(19) (a) Flanagan, J. B.; Margel, S.; Bard, A. J.; Anson, F. C. *J. Am. Chem. Soc.* **1978**, *100*, 4248–4253. (b) Bard, A. J.; Faulkner, R. L. *Electrochemical Methods*, 2nd ed.; Wiley: New York, 2001. (c) Abruna, H. D. In *Electroresponsive Molecular and Polymer Systems*; Stotheim, T. A. Ed.; Dekker: New York, 1988; Vol. 1, p 97. (d) Murray, R. D. In *Molecular Design of Electrode Surfaces*; Techniques of Chemistry XII, Wiley: New York, 1992; p 1. (e) Yamada, M.; Quiros, I.; Mizutani, J.; Kubo, K.; Nishihara, I. *Phys. Chem. Chem. Phys.* **2001**, *3*, 3377–3383.

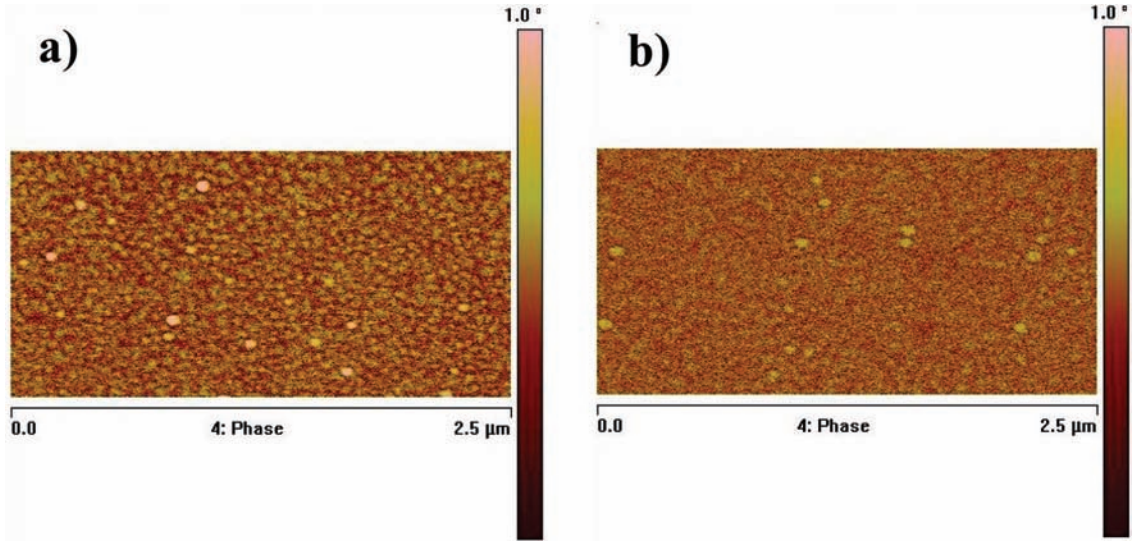

Figure 10. EFM images of (a) solution of the oxidized dendrimer G_5-Fc^+ (left); (b) solution of equimolar G_5-Fc and G_5-Fc^+ (right).

The oxidized form of G_5-Fc was also characterized by AFM in order to compare the size of the cationic form with that of the neutral form. It was found that the average height obtained for the G_5-Fc^+ (6.5 ± 0.6 nm) is much larger than that of its neutral form (4.5 ± 0.4 nm). This experimental difference must be considered with caution, because the type of force that is measured for the neutral ferrocenyl dendrimer is different of the one that is measured by EFM for the ferrocenium dendrimer. On the other hand, this difference can be expected from the repulsive forces between the charged termini in the oxidized dendrimer. Also, in the solid state, the ferrocenium cation forms, with the anion BF_4^-, contact ion pairs[22b] located at the periphery of the dendrimers. The counteranion adds bulk that still increases the dendrimer size, which contributes to the observed large size difference. Thus, these giant redox metallodendrimers exhibit a "breathing mechanism" controlled by the redox potential (Figure 7). In CH_2Cl_2, a solvent that favors ion pairing, this breathing is accompanied by a displacement of the anions from the oxidant toward all the redox termini of the dendrimer, and the opposite is occurring upon reduction of the ferrocenium dendrimer. In an aqueous solvent, the formation of solvent-separated ion pairs would also be accompanied by a large size increase upon oxidation because of the solvation of each ferrocenium termini by several solvent molecules in addition to increased repulsion among the peripheral positive charges.

The pentamethylferrocenyl dendrimers were oxidized using a stoichiometric amount of ferrocenium hexafluorophosphate $[FeCp_2][PF_6]$,[20a] in dry dichloromethane at room temperature for 5 min. After washing the oxidized dendrimers with ether in order to remove the ferrocene formed, they were isolated as green solids and characterized by UV−vis. spectroscopy, showing two absorption bands at 624 and 745 nm (Figure 8). The reduction of the pentamethylferrocenium dendrimers was carried out with an aqueous $TiCl_3$[20a] solution. The pentamethylferrocenyl dendrimers series was thus shown to be highly stable in both the oxidized and reduced forms by quantitative interconversion, their structure being confirmed by ^1H NMR after a complete oxidoreduction cycle.

5. Mixed Valence in Redox Dendrimers. Mixed valence complexes have been extensively investigated since Henry Taube's work because of their particular properties in molecular electronics.[21] Extension to multinuclear ferrocenyl complexes and dendrimer chemistry was emphasized by Casado et al. with mixed-valence dendrimers by cyclic voltammetry. In this case, the short distance between the two ferrocenyl groups induced an electrostatic factor and eventually an electronic communication between them, the superposition of these two significant factors causing a potential difference with two distinct waves in cyclic voltammetry.[22] Our interest now is to discuss the mixed-valence problem in dendrimers in which the redox termini are almost independent because of the large number of σ-bonds between them. Under these conditions, there is no through-bond electronic communication between the redox centers. Also, the redox potentials of the various redox centers are extremely close to one another, because the electrostatic factor is almost nil. What remains, however, is the entropic factor that was highlighted by Suttin and Taube[23] in the expression of the different factors that are involved in mixed valency. This factor is a statistic one, i.e., the various potentials of the redox sites of a dendrimer are provided by a binomial law around a mean value. This distribution is represented in Figure 9 for the half-oxidized dendrimer G_0-Fc containing nine ferrocenyl branches. The ideal cyclic voltammogram is identical to that of a single electron transfer in a monoredox-site compound as discussed in the cyclic voltammetry section, and the redox potentials of all the redox sites of the dendrimers are statistically distributed along this cyclic voltammetry curve.[19]

The oxidized dendrimer G_0-Fc^+ (blue) was mixed with a stoichiometric amount of its G_0-Fc in neutral form (orange) in dichloromethane and the resulting solution of half-oxidized presents a deep green color (eq. 11).

(20) (a) Connelly, N. G.; Geiger, W. E. *Chem. Rev.* **1996**, *2*, 877–910. (b) Geiger, W. E. *Organometallics* **2007**, *26*, 5738–5765 (a historical and perspective article)

(21) Creuz, C.; Taube, H. *J. Am. Chem. Soc.* **1969**, *91*, 3988–3989.

(22) Taube, H. *Angew. Chem., Int. Ed.* **1984**, *23*, 329–339 (Nobel lecture). (a) Cuadrado, I.; Casado, C. M.; Alonso, B.; Móran, M.; Losada, J.; Belsky, V. *J. Am. Chem. Soc.* **1997**, *32*, 7613–7614. (b) Loupy, A.; Tchoubar, B.; Astruc, D. *Chem. Rev.* **1992**, *92*, 1141–1165.

(23) (a) Taube, H. *Electron-Transfer Reactions of Complex Ions in Solution*; Academic Press: New York, 1970. (b) Astruc, D. *Electron-Transfer and Radical Processes in Transition Metal Chemistry*; VCH: Weinheim, Germany, 1995; Chapter 1.

As described by Henry Taube[23] when the two species Fe^{II} and Fe^{III} are together in solution, there is a fast electron transfer among all the redox centers. Thus, applying this statement to dendrimers, we assume that once both forms are mixed in solution, a statistical distribution of mixed-valence dendrimers is obtained with Fe^{II} and Fe^{III} (eq 11 and Figure 9). The presence of mixed-valence dendrimers in such

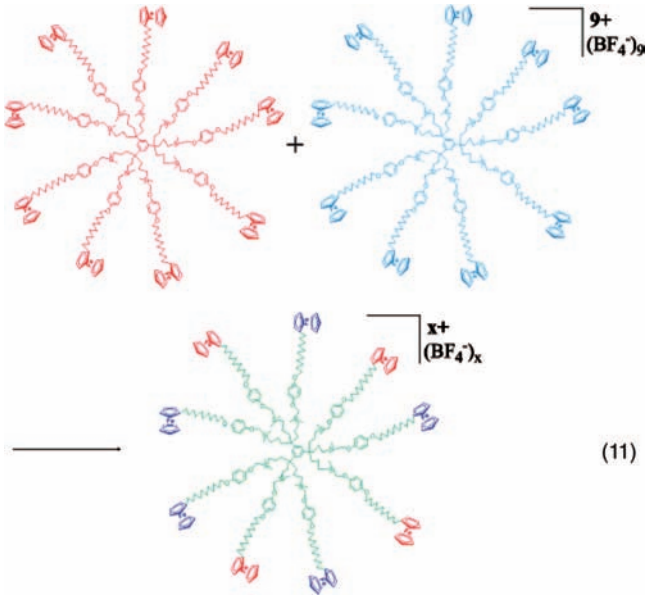

a mixture could be confirmed using the EFM technique (electron force microscopy). With this technique, the nanomolecules that possess a charge density can be distinguished. Thus, a mixture containing equal molar amounts of G_5-Fc and its corresponding oxidized form G_5-Fc^+ were characterized by EFM, and it could be observed that all the nanomolecules present in the images have a charge density with a value, on average, of half (0.44) of the charge density of a pure solution of G_5-Fc^+ (0.82) (all the analyzed spots present, in both cases, similar heights). This is clear evidence for the presence of mixed-valence dendrimers (Figure 10).

Conclusion

The metallodendrimers reported here have high redox stability and could be isolated and characterized in oxidized, reduced and mixed-valence forms. Their size progression was followed from the zeroth to the seventh generation by DLS, AFM, UV−vis, coulometry, and cyclic voltammetry. UV−vis spectroscopy and coulometry show that the defect amount increases as the generation number increases (as expected in classic divergent construction) and reaches 20−30% of the theoretical number of ferrocenyl termini at the seventh generation, i.e., the largest dendrimers somewhat resemble hyperbranched polymers. Finally, however, it has been possible to reach a number of about 14000 ferrocenyl termini whereby, in spite of the strong adsorption, cyclic voltammetry still shows fast electron transfer because of an electron-hopping mechanism. The large amount of defects in G_7 does not perturb this electrochemical reversibility. This strong adsorption of giant ferrocenyl dendrimers should prove very useful for the design of recoverable redox sensors. AFM shows an atom-like quite monodisperse aggregation and the breathing upon redox switching, whereas EFM shows the charged and half-oxidized, mixed-valent systems. All these synthesis, characterizations and stability tests have extended the redox properties of the ferrocenyl and pentamethylferrocenyl complexes to the nanoscale. Thus, these nanomolecules have potential applications in nanoelectronics, such as molecular batteries, capacitors, anion sensors with modified Pt electrodes and electrochromes, because they are highly colored and able to very rapidly transfer a large number of electrons at once (14 000 electrons for G_7) (eqs 12 and 13).

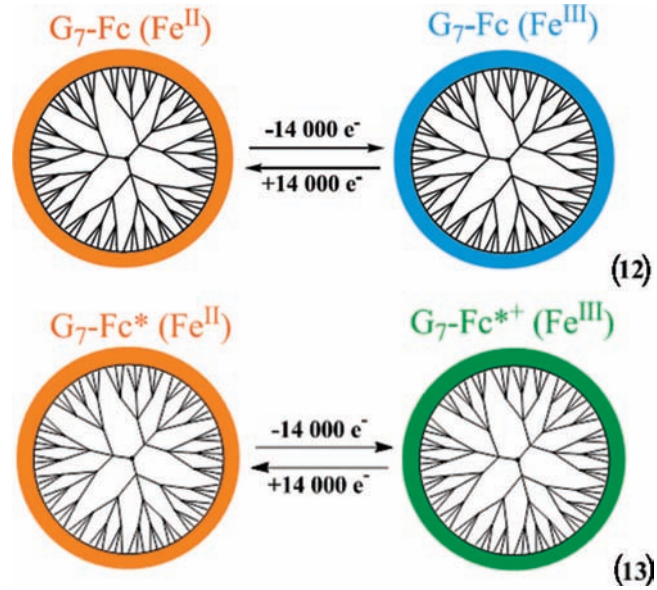

Experimental Section

General Data. For general data including solvents, compounds and reactions, NMR spectroscopy, MALDI TOF mass spectrometry, cyclic voltammetry including modified Pt electrodes and elemental analysis, see the Supporting Information.

Dynamic Light Scattering Measurements (DLS). The DLS measurements were made using a Malvern Zetasizer 3000 HSA instrument at an angle of 90°, in methylene chloride solution at 25 °C. Measurements were carried out at different concentrations until the hydrodynamic diameter was found to be constant at three different concentrations (for high concentration, higher hydrodynamic diameter values were found because of aggregation).

Atomic Force Microscopy (AFM) and Electron Force Microscopy (EFM) Experiments. AFM samples were prepared by spin-coating of a suitable solution (adjusted on trial-error basis) of dendrimer in diethyl ether. Before spin coating, the mica surface was cleaved with Scotch tape. The freshly cleaved highly oriented mica was covered with the solution and spinned at 1000 rpm with subsequent 10−15 s extra spinning at 3000 rpm for complete drying in air. The AFM apparatus is a Thermomicroscope CP Research capable of measurements in multiple modes and the sample imaging is done in air immediately after spin-coating. The noncontact or NC dynamic mode was used giving the weakest interaction with the surface and therefore the less chance of alteration. The cantilever/tip systems used were either Ultralever or Nanosensors, with typical tip (silicon tip) radius of curvature of 10 nm. The amplitude and phase imaging of this mode were used. A sample was considered as good when a monolayer of dendrimers was measured by AFM.

General Synthesis of Ferrocenyl Dendrimers. The iodomethylsilane-dendrimer, **14** (2 equiv. per branch) and K_2CO_3 (10 equiv. *per* branch) were introduced into a Schlenk flask, then dry DMF (30 mL) was added, and the reaction mixture was heated at 80 °C for 48 h under magnetic stirring. After the solvent was removed in vacuo, dichloromethane was added and the mixture was filtered on celite to remove K_2CO_3. The solvent was removed in vacuo and the residue was washed with methanol (2 × 10 mL and

precipitated with CH_2Cl_2/MeOH. After drying in vacuo, ferrocenyl dendrimers were obtained as yellow waxy products. For details concerning each generation, see the Supporting Information and the example of G_5-Fc below.

Synthesis of G_5-Fc, 20. The G_5-Fc dendrimer **20** was synthesized from 2187-iodide dendrimer **7** (0.107 g, 0.000140 mmol), **14** (0.275 g, 0.614 mmol), and K_2CO_3 (0.392 g, 2.80 mmol) using the general synthesis for ferrocenyl dendrimers. The product **20** was obtained as a yellow waxy product in 77% yield (0.158 g, 0.000108 mmol). ^{1}H NMR ($CDCl_3$, 300 MHz), δ: 7.13 (d, arom), 6.80 (m, arom), 4.08 (t, Cp), 3.86 (t, CH_2CH_2O), 3.51 (s, inner $SiCH_2O$), 3.45 (s, outer $SiCH_2O$), 2.31 (t, CH_2Cp), 1.72 (t, CH_2CH_2O), 1.61 (s, $CH_2CH_2CH_2Si$), 1.29 (s, $Cp(CH_2)_8$), 1.13 (s, $CH_2CH_2CH_2Si$), 0.56 (s, $CH_2CH_2CH_2Si$), 0.033 (s, $Si(CH_3)_2$). ^{13}C NMR ($CDCl_3$, 62 MHz), δ: 159.0 (inner $SiCH_2OC_{Ar}$), 155.7 (arom. $CO(CH_2)_{11}$), 153.0 (arom. $COCH_2Si$), 139.2 (arom. C_q), 127.2 and 113.4 (arene *C*H of the dendron), 115.3 and 114.8 (arom. *C*H), 89.5 (*C*q of Cp), 68.4 and 68.0 (Cp), 67.0 ($O(CH_2)_{11}$), 60.9 (OCH_2Si), 43.0 ($CH_2CH_2CH_2Si$), 42.0 (benzylic *C*q), 31.1 (OCH_2CH_2), 29.6 ($(CH_2)_8$), 26.1 ($CpCH_2$), 17.7 ($CH_2CH_2CH_2Si$), 14.6 ($CH_2CH_2CH_2Si$), −4.6 ($Si(CH_3)_2$). ^{29}Si NMR ($CDCl_3$, 59.62 MHz), δ: 0.46 and 0.24 ($Si(CH_3)_2$). Anal. Calcd for $C_{86337}H_{126768}O_{5463}Si_{3276}Fe_{2187}$: C, 70.72; H, 8.71. Found: C, 70.09; H, 9.01.

General Synthesis of Pentamethylferrocenyl Dendrimers. The iodomethylsilane dendrimer, **28** (2 equiv. per branch) and K_2CO_3 (10 equiv. per branch) were introduced into a Schlenk flask, then dry DMF (30 mL) was added and the reaction mixture was heated at 80 °C for 48 h under magnetic stirring. After removing the solvent in vacuo, CH_2Cl_2 (20 mL) was added and the mixture was filtered on celite to remove K_2CO_3. The solvent was removed in vacuo and the residue was washed with methanol (2 × 10 mL) and precipitated with CH_2Cl_2/MeOH. After being dried in vacuo, pentamethylferrocenyl dendrimers were obtained as yellow waxy products. For all details concerning the synthesis of **28** and its precursors, see the Supporting Information.

Synthesis of G_0-Fc*, 29. The G_0-Fc* dendrimer **29** was synthesized from 9-iodide dendrimer **2** (0.050 g, 0.022 mmol), **28** (0.224 g, 0.307 mmol) and K_2CO_3 (0.276 g, 1.97 mmol) using the general synthesis for the pentamethylferrocenyl dendrimers. The dendrimer **29** was obtained as a brown waxy product in 79% yield (0.110 g). ^{1}H NMR ($CDCl_3$, 300 MHz), δ: 7.05 (s, 3H, C*H* core), 6.87 (d, 36H, arom), 3.62 and 3.53 (d, 36H, Cp), 3.54 and 3.51 (d, 36H, $SiCH_2O$), 2.21 (t, 18H, CH_2Cp), 1.90 (s, 135H, CH_3 of Cp*), 1.69 (s, 36H, $CH_2CH_2CH_2Si$), 1.30 (m, 126H, $(CH_2)_7$), 1.25 (s, 36H, $CH_2CH_2CH_2Si$), 0.69 (s, 36H, $CH_2CH_2CH_2Si$), 0.15 and 0.085 (d, 108H, $Si(CH_3)_2$). ^{13}C NMR (CH_3COCH_3, 62 MHz), δ: 155.6 (arom. C_q), 114.2 (arom. *C*H), 88.5 (C_q of Cp), 79.9 (C_q of Cp*), 71.4 and 70.8 (*C*H of Cp), 60.9 (OCH_2Si), 44.0 (benzylic C_q of the core), 33.6 ($CH_2CH_2CH_2Si$), 32.0 ($CpCH_2$), 29.7 ($(CH_2)_7$), 23.7 ($CH_2CH_2CH_2Si$), 13.8 ($CH_2CH_2CH_2Si$), 11.2 (CH_3 of Cp*), −4.64 ($Si(CH_3)_2$). ^{29}Si NMR ($CDCl_3$, 59.62 MHz), δ: 0.45 and 0.32 ($Si(CH_3)_2$). MS (MALDI-TOF; *m*/*z*): Calcd for $C_{378}H_{606}O_{18}Si_{18}Fe_9$, 6647.1; found, 6450.30. Anal. Calcd for $C_{378}H_{606}O_{18}Si_{18}Fe_9$: C, 70.42; H, 9.47. Found: C, 69.78; H, 9.83.

Synthesis of G_7-Fc*, 30. The G_7-Fc* dendrimer **30** was synthesized from 19683-iodide dendrimer **9** (0.050 g, 7.9×10^{-6} mmol) using the general synthesis for the pentamethylferrocenyl dendrimers. The dendrimer **30** was obtained as a brown waxy product in 51% yield (0.073 g). ^{1}H NMR ($CDCl_3$, 300 MHz), δ: 6.86 (m, arom), 3.57 and 3.48 (m, Cp and $SiCH_2O$), 2.16 (t, CH_2Cp), 1.87 (s, CH_3 of Cp* and $CH_2CH_2CH_2Si$), 1.25 (m, $(CH_2)_7$ and $CH_2CH_2CH_2Si$), 0.64 (s, $CH_2CH_2CH_2Si$), 0.075 (d, $Si(CH_3)_2$). ^{13}C NMR (CH_3COCH_3, 62 MHz), δ: 155.6 (arom. C_q), 114.6 (arom. *C*H), 88.4 (*C*q of Cp), 79.8 (C_q of Cp*), 71.3 and 70.7 (*C*H of Cp), 60.9 (OCH_2Si), 33.6 ($CH_2CH_2CH_2Si$), 32.0 ($CpCH_2$), 29.7 ($(CH_2)_7$), 23.7 ($CH_2CH_2CH_2Si$), 13.8 ($CH_2CH_2CH_2Si$), 11.1 (CH_3 of Cp*), −4.7 ($Si(CH_3)_2$). ^{29}Si NMR ($CDCl_3$, 59.62 MHz), δ: 0.43 ($Si(CH_3)_2$). Anal. Calcd for $C_{934893}H_{1495830}O_{49203}Si_{49203}Fe_{19683}$: C, 70.16; H, 9.42. Found: C, 67.78; H, 9.23.

Acknowledgment. Financial support from the Fundação para a Ciência e a Tecnologia (FCT), Portugal (PhD grant to CO), the Institut Universitaire de France (IUF, DA), the University Bordeaux 1, the Centre National de la Recherche Scientifique (CNRS), and the Agence Nationale de la Recherche (Project ANR-06-NANO-026) is gratefully acknowledged.

Supporting Information Available: General data, description of the electrochemical techniques, detailed experimental procedures of the syntheses and characterizations of the metallocene precursors and metallocene dendrimers, and MALDI-TOF mass and NMR spectra (PDF). This material is available free of charge via the Internet at http://pubs.acs.org.

JA8062343